Available online at www.sciencedirect.com
ScienceDirect
Sensors and Actuators A 144 (2008) 213–221
SENSORS AND ACTUATORS A PHYSICAL
www.elsevier.com/locate/sna

Development and experimental characterization of micromachined electromagnetic probes for biological manipulation and stimulation applications

Murat K. Yapici [a,*], Ali E. Ozmetin [b], Jun Zou [a,*], Donald G. Naugle [b]

[a] *Department of Electrical and Computer Engineering, Texas A&M University, College Station, TX 77843, USA*
[b] *Department of Physics, Texas A&M University, College Station, TX 77843, USA*

Received 30 June 2007; received in revised form 9 December 2007; accepted 27 December 2007
Available online 10 January 2008

Abstract

We present the design, fabrication and experimental characterization of a new micromachined electromagnetic probe, which can be readily adapted to various biological manipulation and stimulation applications. The micro electromagnetic probe consists of a protruding (out-of-chip), sharp Permalloy needle embedded into a three-dimensional gold conducting coil. The probe fabrication is carried out using traditional surface micromachining processes coupled with assembly techniques. This hybrid approach significantly reduces fabrication difficulties and provides a simple and straightforward technique to realize integrated core-coil geometries. Furthermore, by using a scanning Hall probe microscope (SHPM), a comprehensive, high-spatial resolution characterization of the probe performance (e.g. peak magnetic intensity and spatial field distribution) is achieved for the first time. The manipulation of sub-micron sized magnetic particles with the developed micro electromagnetic probe is also demonstrated.

Keywords: Micromachined electromagnetic probe; Magnetic manipulation; Transcranial magnetic stimulation; Scanning Hall probe microscope; Magnetic field measurement

1. Introduction

Today, the use of static or time-varying magnetic fields has attracted considerable attention in both *in-vivo* and *in-vitro* biomedical studies. For example, static or quasi-static magnetic fields have been widely used to achieve efficient manipulation and sorting of micro scale particles or biomolecules in "lab-on-a-chip" applications [1–9]. In neuroscience, human cranial stimulation with time-varying magnetic fields has been investigated to serve as a possible non-invasive therapy for certain psychological disorders, such as depression [10–12]. Recent studies have also shown that low-field magnetic stimulation (LFMS) of intensity less than 10 Gauss could change receptor binding parameters in brain membranes [13,14] and produce antidepressant-like effects [15,16]. However, the exact cellular mechanism behind the magnetic neural stimulation method is not well understood and requires further investigation in a more quantitative way [11,14–18].

For the above applications, a localized, concentrated and spatially reconfigurable magnetic field is necessary to achieve precise and selective manipulation or stimulation in a controllable manner [2,19]. Such magnetic fields could be achieved by using a micro electromagnetic probe consisting of a solenoid conducting coil for magnetic field generation and a protruding magnetic core with a sharp tip for magnetic field concentration [20,21]. Once fabricated, the micro electromagnetic probe can be readily used with a micro manipulator to deliver localized magnetic field at any location where it is needed, while the intensity and frequency of the magnetic field can be easily adjusted by changing the input driving current.

However, several technical challenges still remain in the development of micro scale electromagnetic probes. First, due to its small size and complex three-dimensional (3D) structure, the probe fabrication turns out to be complicated and

* Corresponding authors at: Department of Electrical and Computer Engineering, Texas A&M University, 214 Zachry Engineering Center, College Station, TX 77843, USA. Tel.: +1 979 862 1640.
E-mail addresses: mkyapici@tamu.edu (M.K. Yapici), junzou@ece.tamu.edu (J. Zou).

0924-4247/$ – see front matter © 2008 Elsevier B.V. All rights reserved.
doi:10.1016/j.sna.2007.12.029

difficult to implement. Recently, significant progress has been made in microfabrication and micromachining technologies. However, their capability for creating either 3D or protruding microstructures is still limited. To fabricate the 3D conducting coil, complex fabrication steps involving thick photoresist processing [22] or repeated lithography and electroplating have to be used [23,24]. To form the protruding magnetic core, either dry or wet bulk etching is necessary to remove the substrate material underneath, which would involve harsh chemicals and etching conditions, causing material compatibility issues.

Second, due to the small range and large gradient of the generated magnetic field, it is very difficult to achieve a good experimental characterization of the performance of the electromagnetic probe. Conventional magnetic field measurement tools, such as a Gauss meter, cannot provide the needed spatial resolution and sensitivity for such characterization. As a result, so far the design of micro electromagnetic devices has largely relied on numerical simulation and modeling. Recently, scanning techniques coupled with Hall magnetic sensing devices were employed for the characterization of stray magnetic field emanating from magnetic force microscope tips [25]. Equipped with a Hall probe (with a small sensing aperture) and a high resolution piezoelectric stage, a scanning Hall probe microscope (SHPM) system can achieve the needed sensitivity and spatial resolution for micro scale magnetic field measurement [26], and thus could be adapted to the experimental characterization of micro electromagnetic probes.

In this paper, we present the design, fabrication and experimental characterization of a new micromachined electromagnetic probe. First, by combining surface micromachining and guided micro assembly, the fabrication of the electromagnetic probe has been realized with a simple and straightforward process. Next, by capitalizing upon the recent progress in SHPM, we have successfully achieved a comprehensive experimental characterization of the probe performance (e.g. peak magnetic intensity, spatial field distribution, etc.). To our knowledge, this is the first one of such experiments conducted up to date. The high-spatial-resolution SHPM measurement reveals the minute details of the micro scale magnetic field generated by the electromagnetic probe and thus is capable of providing critical information for the design, evaluation and optimization of micromachined electromagnetic probes. Finally, manipulation of fluorescent dye labeled magnetic particles is also tested as an example to demonstrate the functioning of the developed probe.

2. Device design and simulation

Fig. 1 shows a schematic of the micro electromagnetic probe to be developed. It consists of a supporting substrate, a 3D gold coil and a protruding (Permalloy) magnetic core with a sharp tip. To conduct magnetic manipulation, a magnetic particle is attached to the biological sample, which is exposed to the magnetic field (B) created by the micro electromagnetic probe. Suppose the magnetic particle has a total magnetic moment of m, the magnetic force acting on the particle (which can be considered as a magnetic dipole) can be determined by,

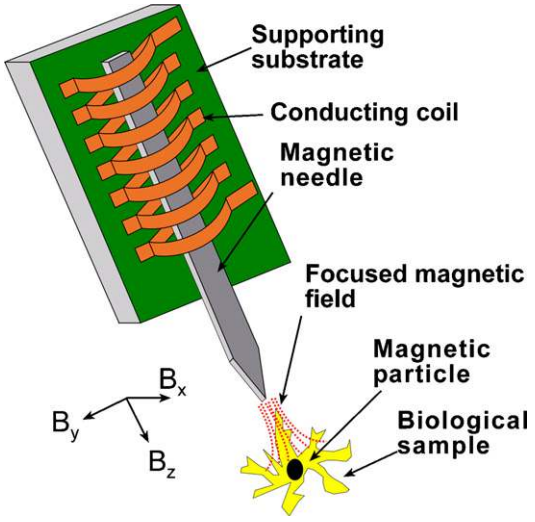

Fig. 1. Schematic of the micro electromagnetic probe to be developed. The probe consists of a supporting substrate, a solenoid conducting coil and a protruding (Permalloy) magnetic core with a sharp tip that allows interaction with biological samples.

$$F = \nabla(m \cdot B) \tag{1}$$

Here, the total magnetic moment m can be expressed as,

$$m = V\chi_m \frac{B}{\mu_0} \tag{2}$$

where χ_m is the volumetric magnetic susceptibility, and V is the volume of the particle [27–29]. Due to the probe geometry, the major component of the magnetization of the magnetic core and thus the magnetic flux from the probe tip will align with the probe axis. Labeling this component of the magnetic flux density as B_z, Eq. (1) can be rewritten as:

$$F = m_z \frac{\partial B_z}{\partial z} = \frac{V\chi_m}{\mu_0}\left(B_z \frac{\partial B_z}{\partial z}\right) \tag{3}$$

According to Eq. (3), the force on a magnetic particle will depend on the volume of the magnetic particle, magnetic susceptibility of the particle material, magnetic flux density, and the gradient of the magnetic flux density. Among these parameters, there is little control on the volume and magnetic susceptibility. The volume of the particles and their magnetic susceptibility are usually small in micro manipulation applications. Therefore, as a main design consideration, the product of the gradient of the magnetic flux density and the magnetic flux density ($B_z(\partial B_z/\partial z)$) should be maximized in order to generate appreciable levels of force or create highly localized magnetic fields which are important for selective manipulation and stimulation.

Since the gradient of the magnetic flux near the probe tip is largely affected by the probe tip profile, the magnetic field generation from different probe tip profiles was simulated using Maxwell 3D® electromagnetic design software. The magnetic properties of the Permalloy core obtained from previous literature [30] were used in the simulation. To simplify the simulation process, the magnetic field generated by the conducting coil

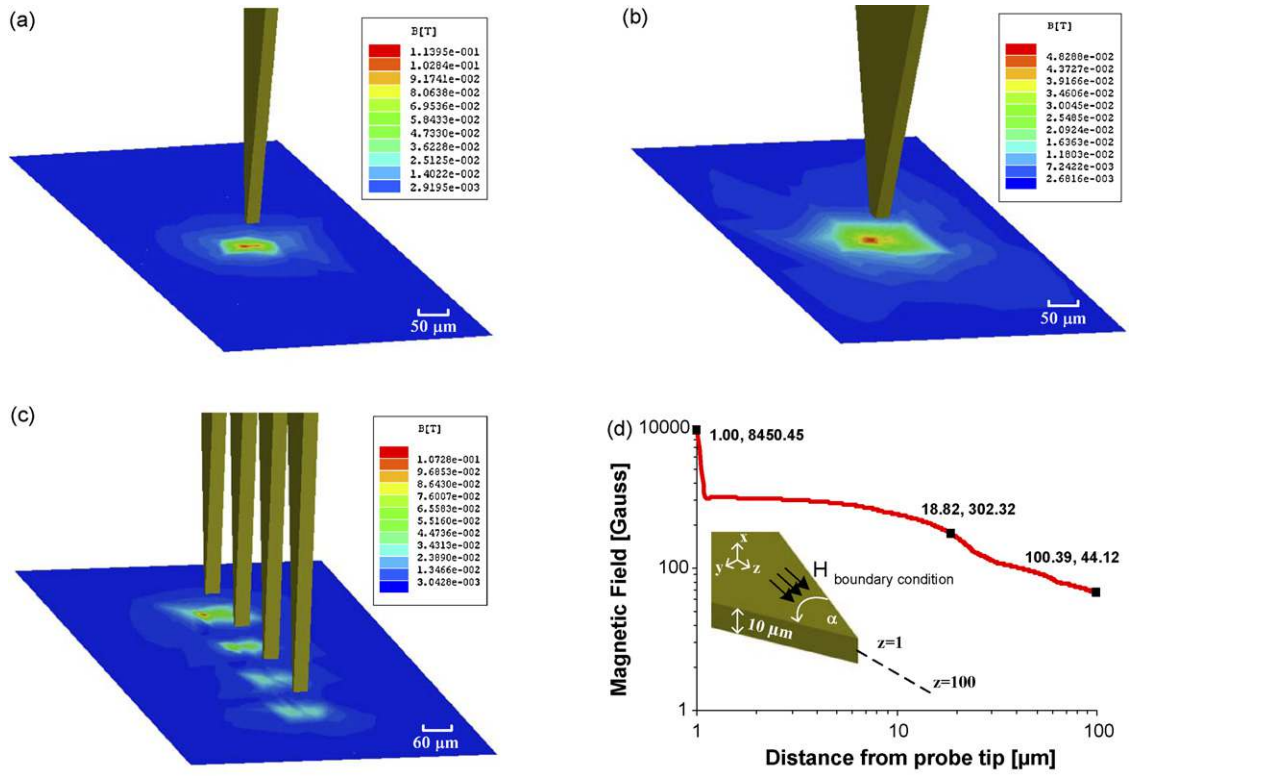

Fig. 2. Simulated magnetic field distribution of different probe tip designs: (a) Field distribution of a probe tip with a taper angle of 15.2°; (b) field distribution of a probe tip with a taper angle of 43.6°; (c) field distribution of a four-tip design; (d) Line plot in log–log scale showing the rapid fall of the magnetic field with respect to distance from the probe tip for a probe design with taper angle 15.2°, shown in the inset is a pictorial representation of the simulation conditions.

was represented with a uniform magnetic field parallel to the axis of the Permalloy core. Different strength of external magnetic field was applied and the magnetization of the Permalloy core was found to be saturated at ∼0.85 T when an external field of 2150 A/m is applied. This field value (2150 A/m) was then imposed as a boundary condition in all the simulations to determine the maximum capability of field generation of different probe designs. Fig. 2(a) and (b) show the magnetic field distribution directly below the probe tips, for two different tip profiles having a taper angle (α) of ∼15.2° and ∼43.6°, respectively. It is clear that smaller taper angle is more effective in creating a higher field concentration. Fig. 2(c) shows the magnetic field distribution for a probe consisting of multiple tips, which indicates that this feature could be used to provide extra flexibility in controlling the magnetic field distribution. Fig. 2(d) shows the field versus distance plot in log scale obtained for a probe design with $\alpha \sim 15.2°$. It is seen that, the bulk Permalloy core region represented by the origin of the log–log plot, reaches the saturation value of ∼0.85 T with the externally applied field of 2150 A/m. Then, during the transition from the Permalloy core to air boundary, the magnetic field starts straying from the tip and due to the difference in relative permeabilities of two medium, an immediate fall in the magnetic field (within a distance of about 100 nm.) is observed. Moving further away from the probe tip causes the magnetic field to fall to a level of ∼30 mT within 20 μm from the probe tip. Based on these results, the gradient of the magnetic flux density was calculated to be on the order of 10^3 T/m which confirms the capability of the proposed device structure to generate large field gradients.

3. Device fabrication

To achieve a simple and straightforward probe fabrication, a hybrid fabrication process involving surface micromachining and guided assembly has been developed, which consists of the three following steps: (1) fabrication of the probe substrates with bottom conductors of the conducting coil; (2) fabrication of the magnetic cores; and (3) assembly of the magnetic core and top conductors of the conducting coil (Fig. 3).

(1) To fabricate the probe substrate with bottom conductors, a layer of chromium (10 nm thick) and gold (300 nm thick) is deposited onto a nitride coated silicon wafer. Gold electroplating with AZ4620 photoresist mold and subsequent etching of the chromium/gold layer are carried out to form the bottom conductors (10 μm thick) of the three-dimensional gold conducting coil. An SU-8 resist layer (10 μm thick) is patterned to provide electrical isolation between the bottom conductor and the magnetic core (to be assembled in Step 3). A second SU-8 layer (50 μm thick) is patterned to form the guiding structures for the assembly of the magnetic core. After the fabrication, the silicon wafer (with different coil designs) is cut into individual dies for subsequent probe assembly (Fig. 3(a)).

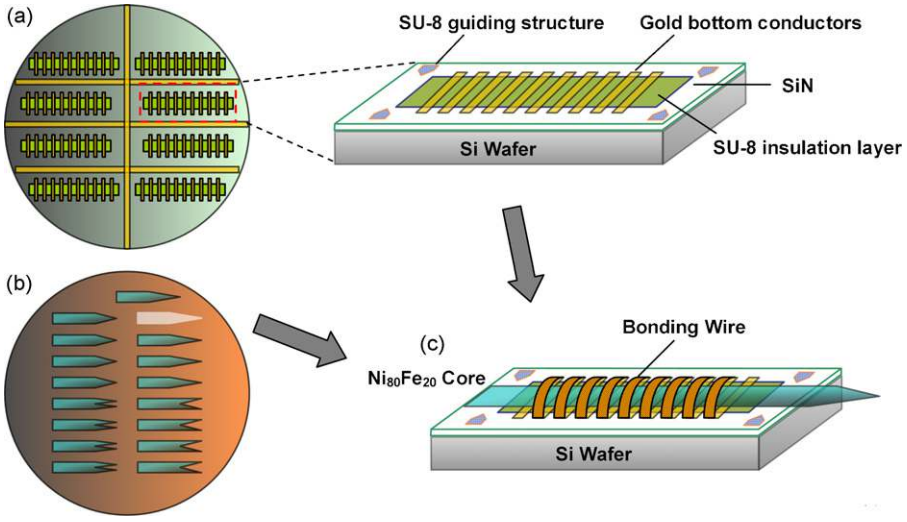

Fig. 3. An illustration of the fabrication process of the micro electromagnetic probe: (a) fabrication of gold bottom conductors and SU-8 insulation and guiding structures; (b) fabrication of the Permalloy magnetic cores; (c) assembly of the magnetic core on the chip and placement of the top conductors with wire bonding.

(2) To fabricate the magnetic core, first a seed layer of chromium (10 nm thick)/copper (300 nm thick) is deposited onto a separate silicon wafer. Permalloy ($Ni_{80}Fe_{20}$) electroplating with AZ4620 photoresist mold is then conducted to form the magnetic core (10 μm thick) of the probe. Once the plating is complete, the AZ4620 mold is completely removed, which is followed by the patterning of an AZ5214 photoresist layer onto each of the Permalloy cores to serve as an insulating layer between the top conductors and the core. Next, electroplated Permalloy cores (with different designs) are released by sacrificial etching of the chromium/copper layer. The micro electromagnetic probe can assume different tip profiles defined by photolithography. This allows the controllable generation of various spatial field distributions for different applications (Fig. 3(b)).

(3) To assemble the entire probe, an electroplated Permalloy core is placed and bonded onto the fabricated silicon chip. The top conductors are placed by gold wire bonding to form a complete 3D conducting coil (Fig. 3(c)). For wire bonding, a suitable wire, which allows a large processing window and operating parameters was selected. We used gold bonding wire of 1 mil (25 μm) in diameter, which is suitable for both wedge and ball bonding and at the same time can provide low loop heights desirable for ideal solenoid formation (Kulicke & Soffa, AW-14 Gold Bonding Wire for Universal Use).

Different conducting coils (width, length and number of turns) and probe tip profiles have been designed and fabricated. The developed fabrication process circumvents the difficulties faced in the direct microfabrication of the 3D conducting coil and the protruding magnetic core, and thus results in a simple and straightforward process. It also offers extra flexibility by allowing the assembly of any combination of conducting coil and magnetic core. The scanning electron micrograph of a fabricated probe is shown in Fig. 4(a). The solenoid consists of 13 turns which span a region of 1.85 mm. The magnetic core has a width of 400 μm, total shank length of 4.75 mm and a tapered extension of 1.5 mm. The probe tip has a taper angle of 15.2°. Fig. 4(b) shows other fabricated Permalloy cores with alternative tip profiles, which could be used for different applications.

4. Experimental characterization

The experimental characterization of the micro electromagnetic probe is achieved using an SHPM system (NanoMagnetics Instruments Ltd.). The experimental test setup depicted in Fig. 5 shows the SHPM stage and the probe assembly designed to

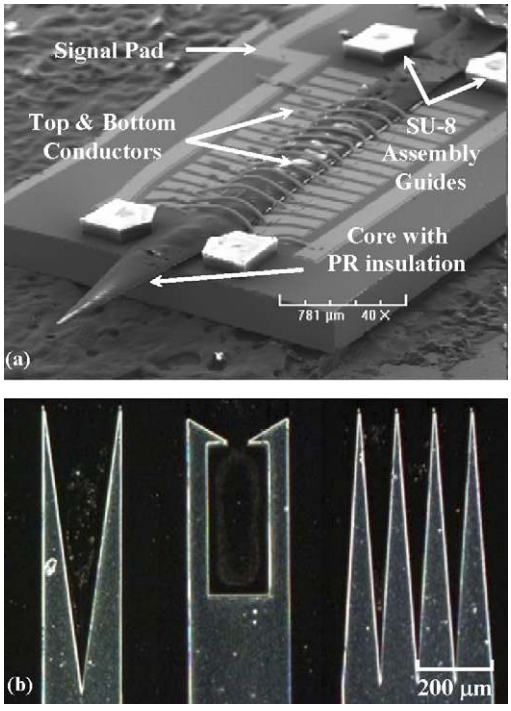

Fig. 4. (a) Scanning electron micrograph of a fabricated micro electromagnetic probe; (b) optical microscopy pictures of Permalloy magnetic cores with different tip profiles.

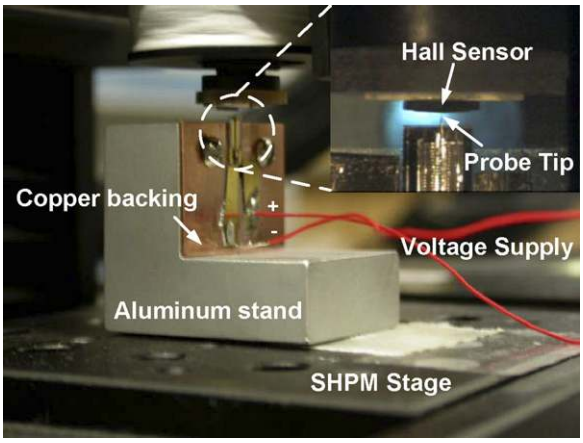

Fig. 5. Scanning Hall probe microscope setup for micro electromagnetic probe characterization. The gap between the probe tip and Hall sensor is estimated to be ~20 μm.

enable efficient testing. The micro electromagnetic probe is attached to a larger copper plate, which facilitates both probe handling and allows rapid dissipation of the heat generated during probe operation. To obtain the temperature distribution on the probe, ANSYS finite element analysis software was used. The plot of the temperature distribution in Fig. 6a indicates that in the case of 300 mA input current to the conducting coil, the maximum temperature on the micro electromagnetic probe is 49 °C, which occurs around the connection points of the bottom and top layer conductors. On the other hand, the maximum temperature on the micro electromagnetic probe tip is 39 °C. Simulations under different input currents were carried out to characterize the effect of input current on the probe temperature. Plot of the tip temperature under different input currents indicates an increasing tip temperature with higher current levels (Fig. 6b). This heat sink mechanism ensures that the Permalloy magnetic cores do not show significant displacement during probe operation, allowing proper testing conditions during characterization experiments and actual operation of the probe in biological applications. The copper plate housing the micro electromagnetic probe is attached to an aluminum stand which allows the probe tip to be easily positioned and aligned perpendicular to the Hall sensor.

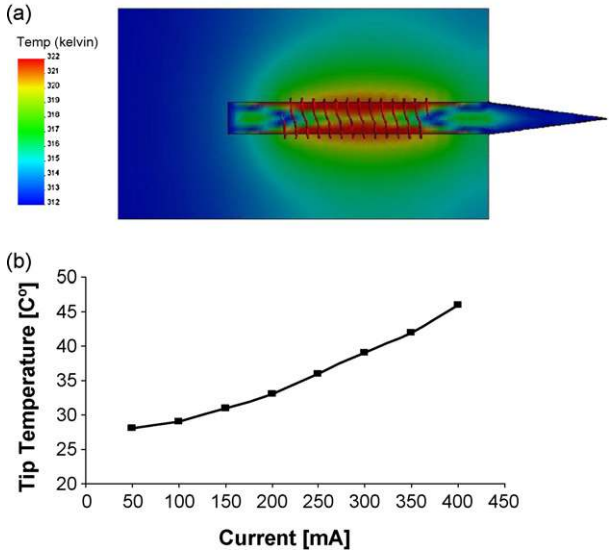

Fig. 6. (a) Finite element simulation showing the temperature distribution on the micro electromagnetic probe under 300 mA input current; (b) plot of the probe tip temperature under different input current levels.

The SHPM is equipped with a Hall sensor probe with a very small sensing aperture (less than 1 × 1 μm) to significantly reduce possible averaging effects in the measurement of the magnetic field. The scanning of the Hall sensor probe is performed by a piezoelectric crystal. The small sensing aperture coupled with the fine scanning step size (100 nm) ensures a high spatial resolution necessary for the probe characterization. To avoid possible collision damage to the Hall sensor, a small gap (~20 μm) is maintained between the Hall sensor element and the probe tip. In this experimental setup, the Hall sensor mainly picks up the magnetic field component parallel to the probe axis (corresponding to B_z in Fig. 1). However, this should not be a big concern in our experiments since B_z is the component of the magnetic field which contributes most to the magnetic manipulation and stimulation of micro scale objects with micro electromagnetic probes.

Before the measurement, the micro electromagnetic probe tip is first demagnetized using the built-in coil of the SHPM by applying an exponentially decaying sinusoidal magnetic field with alternating polarity to the axis of the magnetic core. After the demagnetization, the tip of the micro electromagnetic probe is aligned to the Hall sensor and the peak output magnetic field density (B) as a function of the input current (I) is measured. As shown in Fig. 7, the output magnetic field density (B) first increases linearly as a function of the input current (I) and then saturates around 300 Gauss (30 mT), which is due to the expected ferromagnetic behavior of the core material. Next, the B–H curve of the Permalloy core is obtained, which also reveals a characteristic hysteresis behavior (Fig. 8). It should be noted that the measured saturation intensity of 300 Gauss is much lower than the saturation magnetization of Permalloy (~0.9 Tesla) widely reported in literature [30]. This is because the Hall sensor is positioned around 20 μm away from the probe tip. Due to its large gradient, the magnetic field of the probe will

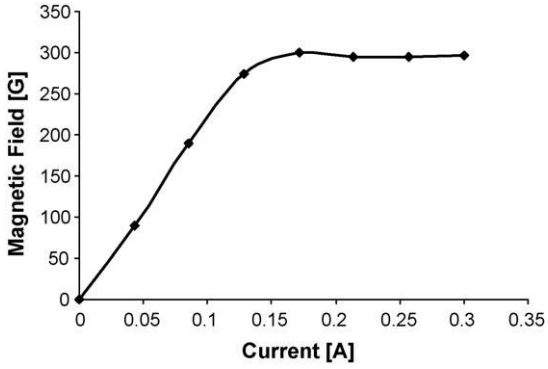

Fig. 7. Magnetic field output 20 μm from the tip of the tested micro electromagnetic probe as a function of input current.

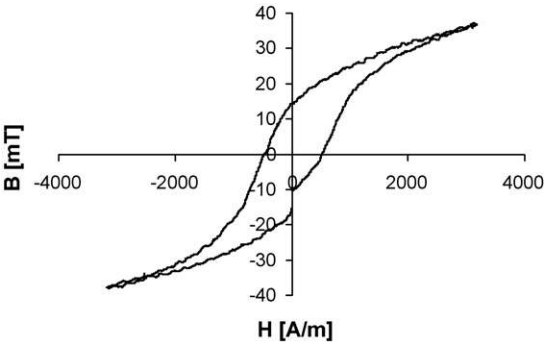

Fig. 8. The *B–H* curve of the Permalloy magnetic core characterized by the scanning Hall probe microscope located about 20 μm from the tip of the core.

quickly diminish at locations farther away from the probe tip. In many biological applications, the samples usually have to be placed at a small distance away from the probe tip. Therefore, our measurement setup and results are valid and useful in assessing the actual magnetic field that will be experienced by the biological samples since they reflect the real working condition of the probes.

In order to obtain the spatial distribution of the magnetic field, the Hall sensor probe is scanned across an area of 25 μm × 25 μm around the probe tip, while maintaining the gap between the probe tip and the Hall sensor. Fig. 9 shows both the axial and the 3D surface plot of the magnetic field distribution when an input current of 300 mA is applied. The field drops rapidly to half of its peak value (297.2 Gauss) within a distance of 4 μm and to a few gauss within a distance of about 12 μm. This translates into large field gradients ($\partial B_z/\partial x = 2768$ T/m and $\partial B_z/\partial y = 2531$ T/m) suitable for biological applications which require site-specific field delivery [1,7,9,28]. On the other hand, the gradient term ($\partial B_z/\partial z$) important for force generation (Eq. (3)) can be found by measuring the magnetic field at two different Hall sensor to probe tip separations. Using this approach, $\partial B_z/\partial$z was calculated to be 2484 T/m, which is similar to the two other gradient components of B_z. This result indicates that the straying of the magnetic field component B_z is almost symmetrical in all three axis.

In our experimental characterization, it is found out that the spatial distribution of the magnetic field is extremely sensitive to the actual profile of the probe tip, which inevitably is different from the design due to imperfection in probe fabrication. This indicates that in applications where an accurate mapping of field distribution is critical, a good experimental characterization is indispensable.

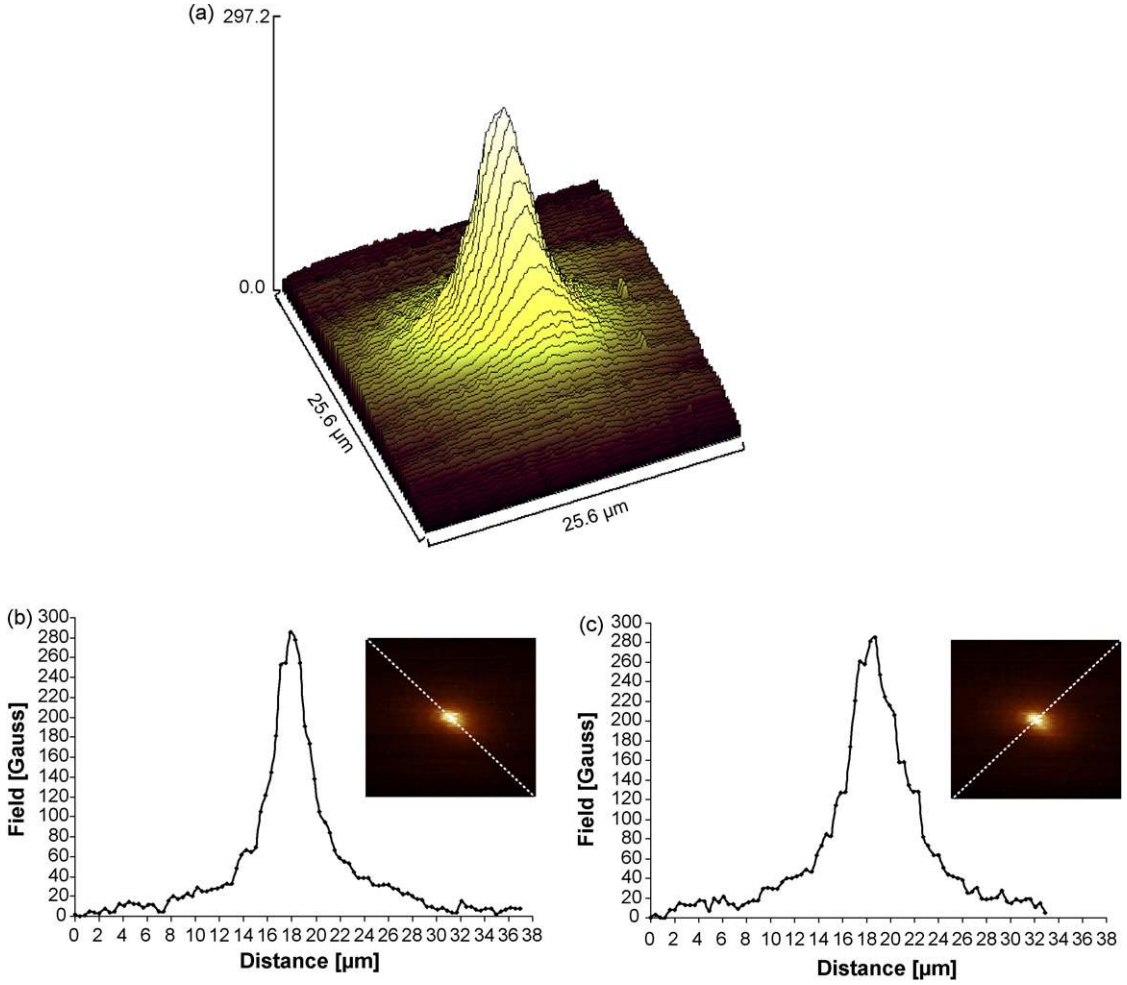

Fig. 9. Measured spatial distribution of the magnetic field output (the component parallel to the axis of the probe) with an input current of 300 mA: (a) surface plot; (b) and (c) axial field plots along the diagonals of the probe tip obtained from the cross-sectional field distribution.

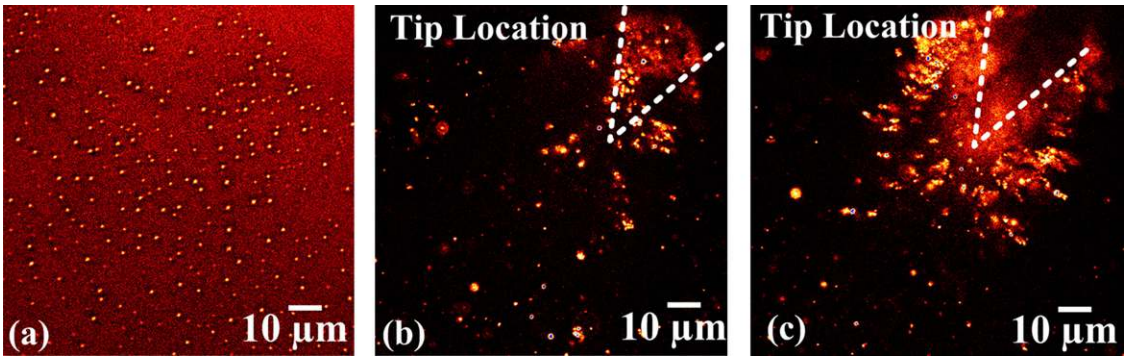

Fig. 10. Manipulation of fluorescent magnetic particles using the developed electromagnetic probe (observed under a fluorescence microscope): (a) Magnetic particles stay in their equilibrium position; (b) and (c) After the probe is turned on, magnetic particles move steadily towards the probe tip.

5. Magnetic particle manipulation

The fabricated micro electromagnetic probe was tested to manipulate fluorescent superparamagnetic particles, which contain 63.4% magnetite and have a spherical shape with mean diameter of 0.9 μm (Bangs Laboratories). Using the values measured with the SHPM for the maximum magnetic field intensity and gradient, and with the magnetic particle susceptibility value (χ_m) of 1.539, forces on the order of several pico newtons (34.52 pN) can be exerted on magnetic particles, and particle manipulation can be achieved.

For the manipulation experiments, in order to avoid rapid evaporation of the water based magnetic particle solution during testing, it was first mixed with glycerol and then a small drop of the mixture was applied on a microscope cover slide. Next, the micro electromagnetic probe with the copper backing is attached to a micro-positioning stage at angle of 40° with the vertical direction.

Manipulation of the magnetic particles was observed under a confocal microscope with 63× immersion lens. Fig. 10a shows the fluorescent magnetic particles at their equilibrium position when the probe was kept above the particle solution with no input current. Fig. 10b and c show the gradual attraction of magnetic particles towards the probe tip after the probe is lowered down using a micro-positioner to contact the liquid surface and an input current of 300 mA is supplied.

In a second experiment, we manipulated a magnetic particle agglomerate to show the capability of moving larger objects in liquid solutions. This capability is important for the manipulation of actual biological entities, such as cells and DNA labeled with magnetic particles [31]. As shown in Fig. 11, initially the probe is off and the particle agglomerate is at rest. When, the probe is turned on with 300 mA input current, the object moves steadily towards the probe tip and is captured within 4 s.

6. Discussion and conclusion

We have demonstrated the design, fabrication and experimental characterization of a new micro electromagnetic probe. By combining surface micromachining and guided assembly to circumvent some of the fundamental challenges in current micromachining technology, a simple, straightforward and versatile probe fabrication has been achieved. With the assistance of the newly-developed robotic systems (e.g. Zyvex® Microgripper system) to perform automated micro manipulation and assembly, an efficient mass production of the micro electromagnetic probes is also possible.

By using an SHPM with high spatial resolution and field sensitivity, a comprehensive experimental characterization of the fabricated probes has been successfully conducted. The experimental measurement technique presented herein allowed real time measurement of magnetic phenomena at the micro scale

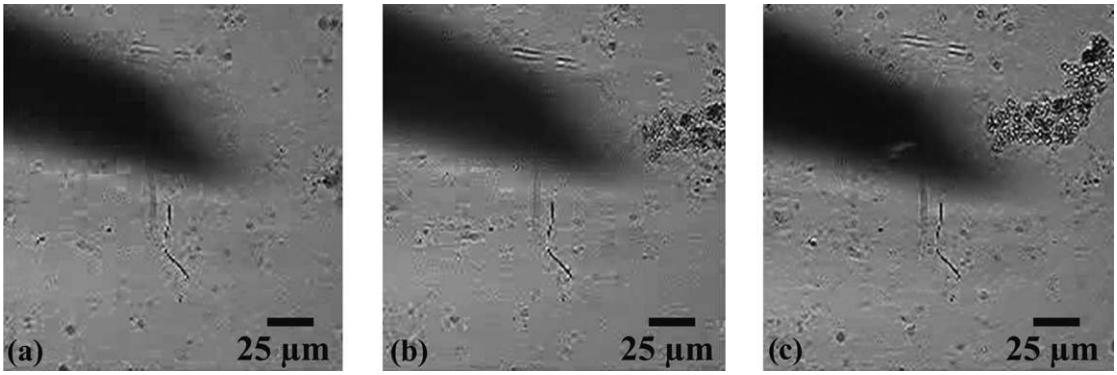

Fig. 11. Manipulation of magnetic particle agglomerate: (a) At $t = 0$ s, magnetic field is applied; (b) At $t = 2$ s, magnetic agglomerate moves toward the probe tip; (c) At $t = 4$ s, magnetic agglomerate is captured.

and provided a venue to evaluate the probe performance for optimized design and application. Results indicate that, further improvement on the probe performance can be achieved through optimizations in the core geometry. For example, fabricating magnetic cores with sharper tips will increase the flux concentration (i.e. magnetic flux density or induction) thereby allowing a higher localization of the field. This can be achieved by using high-resolution pattern generation (e.g. electron beam lithography) or by further sharpening the tips, e.g. with focused ion beam (FIB) etching techniques.

Acknowledgements

This work is partially supported by the Robert A. Welch Foundation, Houston, TX (Grant A-0514) and the National Science Foundation (DMR-0315476). Mr. Fatih Mert Ozkeskin, Texas A&M University, Department of Mechanical Engineering is thanked for his help in thermal FEA simulation.

References

[1] C.S. Lee, H. Lee, R.M. Westervelt, Microelectromagnets for the control of magnetic nanoparticles, Appl. Phys. Lett. 79 (20) (2001) 3308–3310.
[2] T. Deng, G.M. Whitesides, M. Radakrishnan, G. Zabow, M. Prentiss, Manipulation of magnetic microbeads in suspension using micromagnetic systems fabricated with soft lithography, Appl. Phys. Lett. 78 (12) (Mar. 2001) 1775–1777.
[3] H. Lee, A.M. Purdon, R.M. Westervelt, Manipulation of biological cells using a microelectromagnet matrix, Appl. Phys. Lett. 85 (6) (2004) 1063–1065.
[4] H. Lee, A.M. Purdon, V. Chu, R.M. Westervelt, Controlled assembly of magnetic nanoparticles from magnetotactic bacteria using microelectromagnets arrays, Nano Lett. 4 (5) (2004) 995–998.
[5] R. Rong, J.-W. Choi, C.H. Ahn, An on-chip magnetic bead separator for biocell sorting, J. Micromech. Microeng. 16 (Nov. 2006) 2783–2790.
[6] K. Smistrup, P.T. Tang, O. Hansen, M.F. Hansen, Microelectromagnet for magnetic manipulation in lab-on-a-chip systems, J. Magn. Magn. Mater. 300 (2006) 418–426.
[7] N. Pekas, M. Granger, M. Tondra, A. Popple, M.D. Porter, Magnetic particle diverter in an integrated microfluidic format, J. Magn. Magn. Mater. 293 (Mar. 2005) 584–588.
[8] E. Mirowski, J. Moreland, S.E. Russek, M.J. Donahue, Integrated microfluidic isolation platform for magnetic particle manipulation in biological systems, Appl. Phys. Lett. 84 (10) (2004) 1786–1788.
[9] M. Berger, J. Castelino, R. Huang, M. Shah, R.H. Austin, Design of a microfabricated magnetic cell separator, Electrophoresis 22 (18) (2001) 3883–3892.
[10] V. Walsh, A. Cowey, Transcranial magnetic stimulation and cognitive neuroscience, Nature Rev. Neurosci. 1 (2000) 73–79.
[11] C.K. Loo, P.B. Mitchell, A review of the efficacy of transcranial magnetic stimulation (TMS) treatment for depression, and current and future strategies to optimize efficacy, J. Affect. Disord. 88 (2005) 255–267.
[12] M.S. George, E.M. Wassermann, T.A. Kimbrell, J.T. Little, W.E. Williams, A.L. Danielson, B.D. Greenberg, M. Hallett, R.M. Post, Mood improvement following daily left prefrontal repetitive transcranial magnetic stimulation in patients with depression: a placebo-controlled crossover trial, Am. J. Psychiat. 154 (12) (1997) 1752–1756.
[13] O. Massot, B. Grimaldi, J.M. Bailly, M. Kochanek, F. Deschamps, J. Lambrozo, G. Fillion, Magnetic field desensitizes 5-HT_{1B} receptor in brain: pharmacological and functional studies, Brain Res. 858 (1) (Mar. 2000) 143–150.
[14] J.M. Espinosa, M. Liberti, I. Lagroye, B. Veyret, Exposure to AC and DC magnetic fields induces changes in 5-HT_{1B} receptor binding parameters in rat brain membranes, Bioelectromagnetics 27 (2006) 414–422.
[15] M. Rohan, A. Parow, A.L. Stoll, C. Demopulos, S. Friedman, S. Dager, J. Hennen, B.M. Cohen, P.F. Renshaw, Low-field magnetic stimulation in bipolar depression using an MRI-based stimulator, Am. J. Psychiat. 161 (1) (Jan. 2004) 93–98.
[16] W.A. Carlezon, M.L. Rohan, S.D. Mague, E.G. Meloni, A. Parsegian, K. Cayetano, H.C. Tomasiewicz, E.D. Rouse, B.M. Cohen, P.F. Renshaw, Antidepressant-like effects of cranial stimulation within a low-energy magnetic field in rats, Biol. Psychiat. 57 (6) (2005) 571–576.
[17] M.H. Repacholi, B. Greenebaum, Interaction of static and extremely low frequency electric and magnetic fields with living systems: health effects and research needs, Bioelectromagnetics 20 (3) (1999) 133–160.
[18] S.M. Fitzpatrick, D.L. Rothman, Meeting report: transcranial magnetic stimulation and studies of human cognition, J. Cogn. Neurosci. 12 (4) (2000) 704–709.
[19] S. Ueno, T. Tashiro, K. Harada, Localized stimulation of neural tissues in brain by means of a paired configuration of time-varying magnetic fields, J. Appl. Phys. 64 (10) (Nov. 1988) 5862–5864.
[20] M. Barbic, J.J. Mock, A.P. Gray, S. Schultz, Scanning probe electromagnetic tweezers, Appl. Phys. Lett. 79 (12) (2001) 1897–1899.
[21] B.D. Matthews, D.A. LaVan, D.R. Overby, J. Karavitis, D.E. Ingber, Electromagnetic needles with submicron pole tip radii for nanomanipulation of biomolecules and living cells, Appl. Phys. Lett. 85 (14) (2004) 2968–2970.
[22] N. Chomnawang, J.-B. Lee, W.A. Davis, Surface micromachined arch-shape 3D solenoid inductors for high frequency applications, J. Microlith. Microfab. Microsyst. 2 (4) (2003) 275–281.
[23] H. Lu, J.-C. Lee, B. Pillans, K. Kim, J.-B. Lee, High aspect ratio air core solenoid inductors using an improved UV-LIGA process with contrast enhancement material, Microsyst. Technol. 13 (2007) 237–243.
[24] J.-B. Yoon, B.-K. Kim, C.-H. Han, E. Yoon, K. Lee, C.K. Kim, High-performance electroplated solenoid-type integrated inductor (SI^2) for RF applications using simple 3D surface micromachining technology, Proc. IEEE Int. Electron Dev. Meeting (1998) 544–547.
[25] A. Thiaville, L. Belliard, D. Majer, E. Zeldov, J. Miltat, Measurement of the stray field emanating from magnetic force microscope tips by Hall effect microsensors, J. Appl. Phys. 82 (7) (1997) 3182–3191.
[26] A.M. Chang, H.D. Hallen, L. Harriott, H.F. Hess, H.L. Kao, J. Kwo, R.E. Miller, R. Wolfe, J. van der Ziel, T.Y. Chang, Scanning Hall probe microscopy, Appl. Phys. Lett. 61 (16) (1992) 1974–1976.
[27] Q.A. Pankhurst, J. Connolly, S.K. Jones, J. Dobson, Applications of magnetic nanoparticles in biomedicine, J. Phys. D.: Appl. Phys. 36 (Jun. 2003) R167–R181.
[28] C.H. Ahn, M.G. Allen, W. Trimmer, Y.-N. Jun, S. Erramilli, A fully integrated micromachined magnetic particle separator, J. Microelectromech. Syst. 5 (3) (Sept. 1996) 151–158.
[29] C.-H. Chiou, G.-B. Lee, A micromachined DNA manipulation platform for the stretching and rotation of a single DNA molecule, J. Micromech. Microeng. 15 (2005) 109–117.
[30] J.Y. Park, M.G. Allen, Development of magnetic materials and processing techniques applicable to integrated micromagnetic devices, J. Micromech. Microeng. 8 (1998) 307–316.
[31] C.-H. Chiou, Y.-Y. Huang, M.-H. Chiang, H.-H. Lee, G.-B. Lee, New magnetic tweezers for investigation of the mechanical properties of single DNA molecules, Nanotechnology 17 (Feb. 2006) 1217–1224.

Biographies

Murat Kaya Yapici received his BS degree in electrical engineering from Texas A&M University, College Station in 2004, where he is currently pursuing his PhD. Upon joining the department, he worked on developing new micromachining technology for RF microelectromechanical systems. His current research interests lie in the development of micro/nano electromechanical devices and systems for biological applications and novel nano fabrication technology based on scanning probe techniques.

Ali Esad Ozmetin received MS degree in Physics from Texas A&M University, Texas, USA, in 2002. He is currently pursuing a graduate degree at the Physics Department, Materials Engineering Program at Texas A&M University, Texas, USA.

Jun Zou received his PhD. degree in electrical engineering from the University of Illinois at Urbana-Champaign (UIUC) in 2002. From 2002 to 2004, he was a post-doctoral researcher in the Micro and Nanotechnology Laboratory at UIUC. In August 2004, he joined in the department of electrical and computer engineering at Texas A&M University in College Station where he is currently an assistant professor. Dr. Zou's research interests lie in the development of micro and nano opto-electro-mechanical devices and systems as well as novel micro- and nanofabrication methods. Since 1994, he has been conducting interdisciplinary research in this area and successfully developed a number of micromachined devices for applications in microfluidics, acoustics, RF communication and nanotechnology. In 2001, he invented a new micromachining process—Plastic Deformation Magnetic Assembly (PDMA) for efficient fabrication of complicated 3D microstructures. His recent research effort is primarily focused on micro and nano diagnostic and surgical tools for biomedical applications. He has contributed more than 40 peer-reviewed journal and conference publications and holds three US patents. Dr. Zou is a member of IEEE and the IEEE Electron Devices Society.

Donald Naugle completed the BA in Physics at Rice University in 1958. After four years service in the US. Marine Corps, he completed his PhD in Condensed Matter Physics at Texas A&M University in 1965. After a NATO Postdoctoral Fellowship at the University of Goettingen, Germany and postdoctoral study at the University of Maryland, he joined the faculty of Texas A&M University in 1969 and is currently a Professor in the Physics Department there.